



## Contribution to the Turbulent Flow Separation Study in an Asymmetric Subsonic Plane Diffuser by RANS Models

M. Aounallah<sup>1</sup>, O. Madani Fouatih<sup>2</sup>, M. Belkadi<sup>1</sup>, L. Adjlout<sup>1\*</sup>

<sup>1</sup>Laboratoire d'Aéro Hydrodynamique Naval "LAHN" Département de Génie Maritime

<sup>2</sup>Aeronautics and Propulsive Systems Laboratory. Faculté de Génie Mécanique  
Université des Sciences et de la Technologie D'Oran Mohamed BOUDIAF  
BP1505 El M'nouar 31000 Oran Algérie.

\* Corresponding author. [adjloutl@yahoo.fr](mailto:adjloutl@yahoo.fr)

Received. December 19, 2019. Accepted. June 21, 2020. Published. September 22, 2020.

DOI: <https://doi.org/10.58681/ajrt.20040201>

**Abstract.** The present study deals with separate turbulent flow in a 2D subsonic asymmetric plane diffuser using ANSYS Fluent commercial code. Several models of turbulence have been tested namely: the Spalart-Allmaras model, k- $\omega$  SST, feasible k- $\epsilon$  and RSM.

The Spalart-Allmaras and k- $\omega$  SST models provided the best tuning for the 2D case. Instantaneous flow recirculation has been observed along the inclined wall where the average flow profile changes gradually as the flow enters the expansion zone.

The structure of the flow in the asymmetric diffuser, as a function of the variation of the angles and according to different Reynolds numbers, was also analyzed.

The results show that the influence of the size of the recirculation region for a turbulent flow is ambiguous with the variation of the Reynolds number, but evident with the change of angles of the diffuser.

**Keywords.** Separation, Diffuser, Re-attachment, Modeling.

### INTRODUCTION

In fluid mechanics, two of the most important phenomena that are most difficult to predict are separation and re-attachment of flows.

Most numerical computation models find it difficult to predict where the flux separates due to rapid changes in flow, when the flow is connected, and how the boundary layer is subsequently redeveloped.

Separation is important because it occurs in many engineering applications, hence the interest of the diffuser, wings in landing configuration.

In the first two cases, separation is generally not a desirable state, but often accepted in order to meet other constraints.

The separation causes a loss of efficiency in the fluid flow devices, resulting in kinetic and potential energy losses.

The diffuser is an integral part of jet engines and many other devices that depend on fluid flow.

The performance of a propulsion system as a whole depends on the efficiency of the diffusers. The identification of the separation in the diffusers is important because it increases the drag and causes a deformation on the motor fans and on the compressors.

The calculation of the flow in the diffuser is a particularly difficult task for the simulation of fluid dynamics calculations (CFD) due to the adverse pressure gradients created by the slowed flow which often causes the separation, the latter is highly dependent the level of local turbulence, parietal viscous effects and the diffuser pressure ratio.

Several studies have been carried out on geometries inducing a flow separated by an adverse pressure gradient.

However, the study is focused on fully developed turbulent flow in a planar asymmetric diffuser.

Obi et al. (1993) conducted an experimental study of turbulent flow in an asymmetric plane diffuser of  $10^\circ$  and a total expansion ratio of 4.7.

Using a Velocimetry Laser Doppler (LDV), the authors were able to measure the three components of velocity in the diffuser enclosure.

In another article, Obi et al. (1993) continued to study the same flow experimentally disturbed periodically by blowing and suction through a slit in the direction of flow. They studied the influence of the perturbation frequency on the size of the separation bubble. They concluded that at the optimal frequency ( $St = 0.03$ ) of disturbance, the increase in transport of the momentum through the diffuser is maximal.

Buice (1997) also made an experimental investigation on a configuration similar to that of elongated Obi. They found that the flow separated at a distance of  $7H$  and re-attached at  $29H$ .

Tornblom (2003) experimentally studied turbulent flow separation in an asymmetric plane diffuser of  $8^\circ$ .

The velocity field, comprising three components, was traced with the techniques of Particle Image Velocimetry (PIV) and Velocimetry Laser Doppler (LDV).

The results showed that the flow detaches from the inclined wall at a distance approximately equal to 9 times the thickness of the diffuser inlet channel.

This point moves in both directions, but never in front of  $x / H = 5$ . The re-attachment point also fluctuates in the region of the intake channel sizes. On average, this point is at  $x / H = 31$  (Kaltenbach et al., 1999).

An extensive numerical study of the flow in the planar asymmetric diffuser was performed by Kaltenbach et al. (1999), using the simulation of large LES scales for a Reynolds number of about 1,000.

Iaccarino (2000) found that the sub-mesh model is adequate for a correct flow calculation since sub-mesh stresses have a significant and direct contribution to shear stresses at the wall.

Iaccarino (2000) conducted a comparative study of turbulent flow in a flat asymmetric diffuser using three commercial CFD codes: CFX, Fluent and Star-Cd.

Two models of turbulence were used: the Reynolds low-Reynolds model and the  $v2-f$  model. The accuracy of the numerical results compared to the experimental data and numerical results from the LES is very good, using the  $v2-f$  model.

However, the limits of the model  $k - \epsilon$  low Reynolds number are probably visible, the results obtained by the model  $k - \epsilon$  show no separation of the flow (Tornblom, 2003).

## FORMULATION OF THE PROBLEM

The flow that is the subject of this study is a flow in an asymmetric plane diffuser (Fig.1). The interest of this study is to predict the separation and the re-attachment whose positions are not directly related to a sudden change of geometry. As a database, the ERCOFTAC test is a well-documented experimental database (DalBello et al., 2005), where entry conditions are well defined in the experiment conducted by (Buice, 1997).

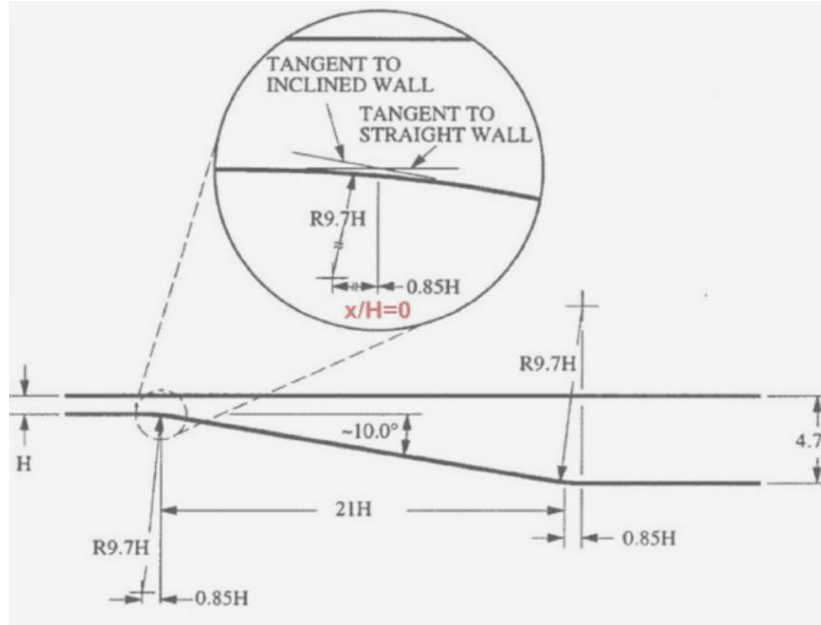


Fig.1. Details on the diffuser geometry (Davidson, 2005).

### General Equations

In order to obtain a simple mathematical model, the following classical approximations are made:

- The fluid is Newtonian and incompressible.
- The flow at the inlet of the channel is fully developed turbulent.
- The flow is stationary.
- The diffuser walls are adiabatic.

In this study, conservation equations for turbulent incompressible fluid flow with constant properties are used.

The governing flow field equations are continuity and momentum equations supplemented by the equations of the turbulence models tested, which are given by:

$$\frac{\partial U_i}{\partial x_i} = 0 \quad i=1,2,3 \quad (1)$$

$$\frac{\partial U_i}{\partial t} = -\frac{1}{\rho} \frac{\partial P}{\partial x_i} + \frac{\partial}{\partial x_j} \left[ (\nu + \nu_t) \frac{\partial U_i}{\partial x_j} \right] \quad (2)$$

### SIMULATION

The numerical simulation of the flow is carried out under Fluent (6.3.26). This is intended to solve the Navier-Stokes equations with a RANS (Reynolds Averaged Navier Stokes) approach. To model the Reynolds stresses that appear in the equations, we can use various models of turbulence: Spalart-Allmaras model, k-omega SST model and the RSM model.

#### 3.1 Generation of the mesh:

To obtain a solution independent of the mesh, a resolution has been studied with a structured two-dimensional mesh (hexahedron) (Fig. 2). Two types of mesh dependency studies have been performed:

- The coarse mesh with  $341 \times 61$ .
- The average mesh with  $341 \times 81$ .
- The fine mesh with  $341 \times 100$ .

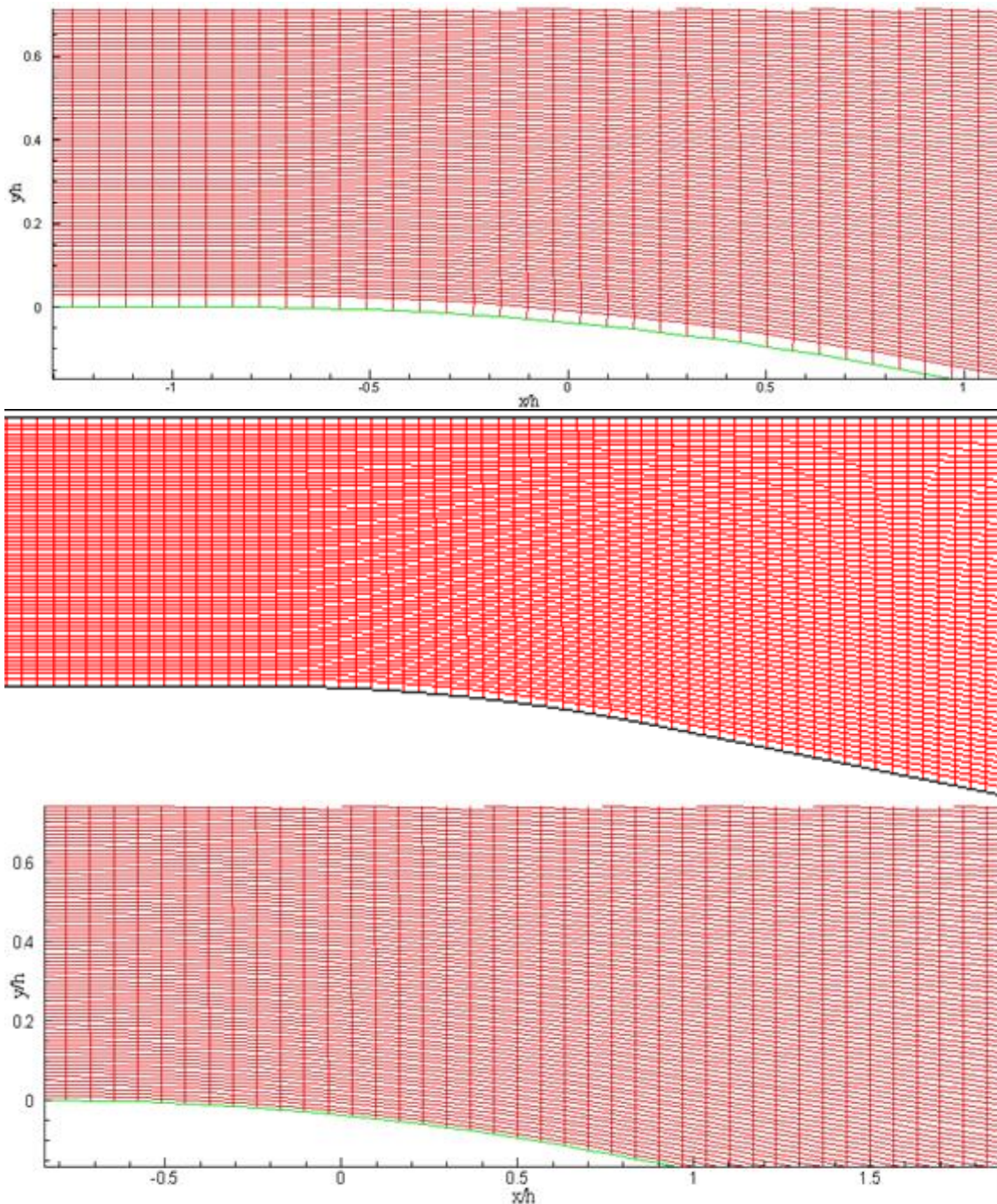


Fig. 2. Mesh resolution representations for different layer thicknesses at the diffuser.

The second mesh dependence study is based on the initial spacing of the wall, it has been modified for each mesh, and it has been extended for different types of meshes with a dimensional value and equal to 5, 15 and 30.

## Boundary conditions

In order to solve the turbulence problem for this problem (ie, the same number of Reynolds).

$$U_{in} = \frac{Re \times \nu}{h} = \frac{20000 \times 1.46735 \times 10^{-5}}{0.0150} = 20 \text{ m/s} \quad (3)$$

This channel used corresponds to the Reynolds number of 20000 defined by the width of the channel and the free stream velocity.

Simulations required by the model to have a developed turbulent flow, and to provide a set of profiles for driving condition specifications, a calculation in the  $2h \times 1h$  size channel was realized. In addition, the resolution of the channel crossing should be identical to the mesh in the inlet area of the asymmetrical diffuser. The boundary conditions for inlet and exit are both indicated as periodic. The periodic condition on the small channel is given by the mass flow calculated as follows:

$$\dot{m} = \rho U_{in} h l = 1.225 \times 20 \times 0.0120 \times 1 = 0.367793 \text{ kg/s} \quad (4)$$

## OPTIMISATION

The calculations are performed for two-dimensional asymmetric diffusers with 4.7. It consists in studying the influence of the speed at the entrance and the angle of enlargement on the separation and the fixation of the fluid particles on the lower wall of the diffuser. The tests were carried out on the Reynolds numbers of 10,000, 15,000, 20,000, 25,000 and 30,000. The angles vary between  $6^\circ$  and  $16^\circ$  with a step of  $2^\circ$ . Two models of turbulence named Spalart-Allmaras and k- $\omega$ SST were chosen in the first part of this study, a mesh size  $100 \times 341$  was adopted.

## RESULTS AND DISCUSSIONS

### Validation of numerical results

The geometry of the diffuser used in the calculations is identical to that used in the Obi et al. experiments (1993) and Buice report (1997). The system of RANS equations is solved with the models: Spalart-Allmaras, Feasible, k- $\epsilon$ , k- $\omega$  SST and RSM in steady state. The following table summarizes the separation and re-attachment positions predicted by the different tested turbulence models.

Table 1 compares the numerical results with those available in the literature. The results show a small difference between the separation points and reattachment points. In general, the reference point is well captured for all models.

The best model is that of k-SST with  $341 \times 81$  and  $y^+ = 15$ , the absolute error is approximately equal to 1%. The prediction of the separation point shows, nevertheless, the unreliability of the models, the location of this point is the value of  $x / h$  equal to 7.4 predicted experimentally.

The nearest predictive value is  $x / h$  equals 5 (Sp-Al  $341 \times 81$ ,  $y^+ = 5$ ), the other models underestimate the start of the separation  $x / h = 2$  for the model k- $\omega$  SST.

The feasible model k- $\epsilon$  underestimates the separation region by providing a smaller and thinner separation bubble.

Table 1. Comparison of results.

Model	Reference (Buice, 1997)	Sp-Al	k- $\omega$ SST	RSM
Separation [x/h]	7.4	5	2	5
Reattachment [x/h]	29.2	31	31	25

Figure 3 shows the longitudinal component of the velocity for the Spalart-Allmaras and K- $\omega$  SST models. Dark blue contours (clearly). Spalart-Allmaras and k- $\omega$  SST are qualitatively in good agreement with experimental measurements.

The sensitivity study of the solution as a function of the variation of the first cell is represented in the figure. 4. Three meshes are tested with the order of the order of 5.15 and 30.

$$y^+ = \frac{y \cdot U \cdot \rho}{\mu} \quad (5)$$

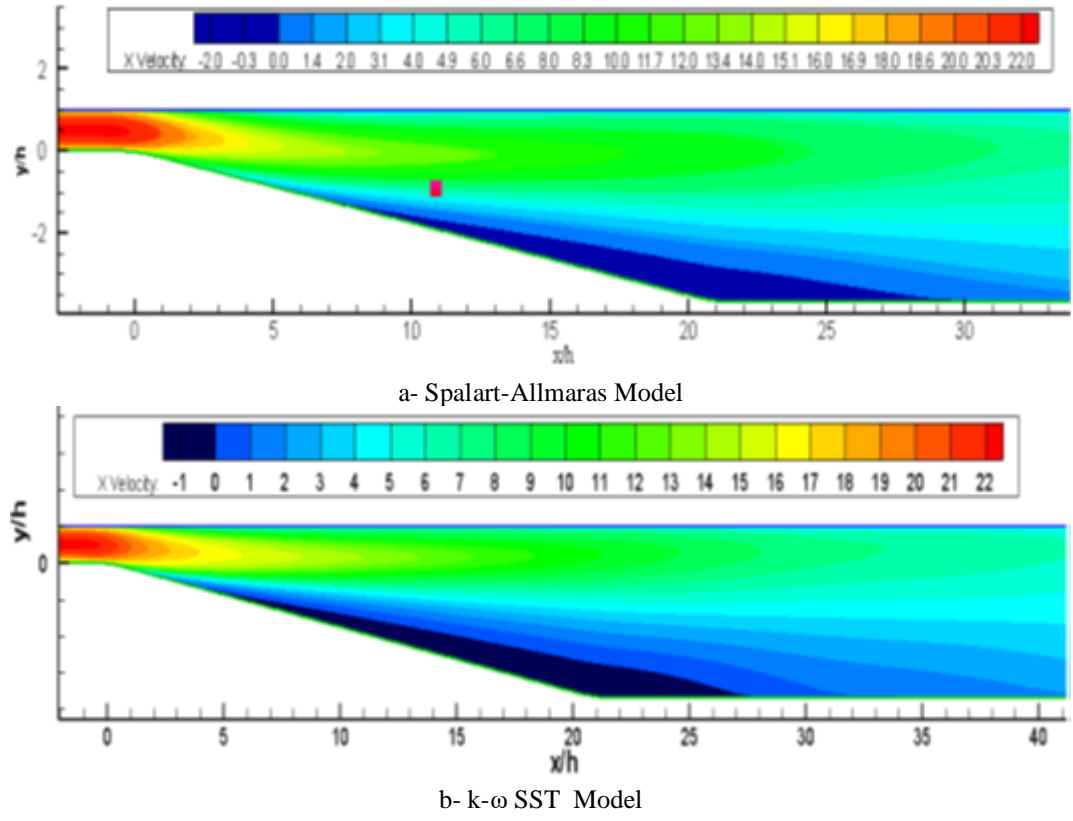


Fig. 3. Axiale vitesse Contour.

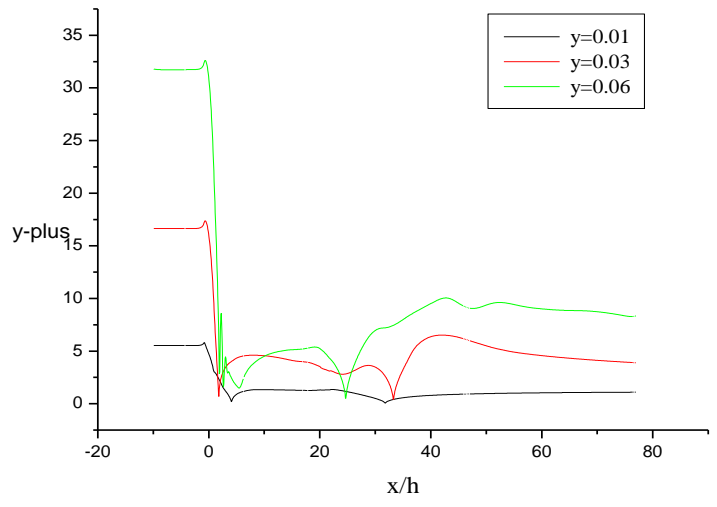


Fig. 4. Distribution of y-plus (y +) for different meshes (Sp-Al model).

The distribution of the coefficient of friction is shown in figure 5. The value of  $C_f$  is used to calculate the initial space at the wall. The value of the coefficient of friction is described as follows:

$$C_f = \frac{\tau_w}{\frac{1}{2} \rho U_b^2} \quad (6)$$

Where is  $\tau_w$  the shear stress defined by:

$$\tau_w \approx \mu \left( \frac{\partial U}{\partial y} \right)_{wall} \quad (7)$$

The comparison shows a slight difference between the experimental coefficient and the coefficients found by the various tested turbulence models.

The results of the simulation of the Spalart-Allmaras model and  $k-\omega$  SST are in good agreement, qualitatively, with all the experienced ones.

The curve of coefficient of parietal friction goes through three stages, it takes the maximum value at the inlet of the diffuser, goes into the expansion zone then in the recirculation zone then it increases gradually.

These values have been reasonably optimized. Similarly, the distribution of this coefficient on the top wall is shown in the figure 5 where it is reported the absence of any separation of the fluid particles.

The  $k-\omega$  SST model seems more appropriate in the expansion zone, whereas the results of the Spalart-Allmaras model are more closer to the experimental in the upstream zone of  $x/h = 40$ .

Figure 6 shows the comparison of the pressure coefficient on the bottom wall for the models tested.

The pressure coefficient obtained with the  $k-\omega$ SST model is reasonably in agreement with the experimental data, while the Sp-Al model gives an overestimated value for the pressure coefficient.

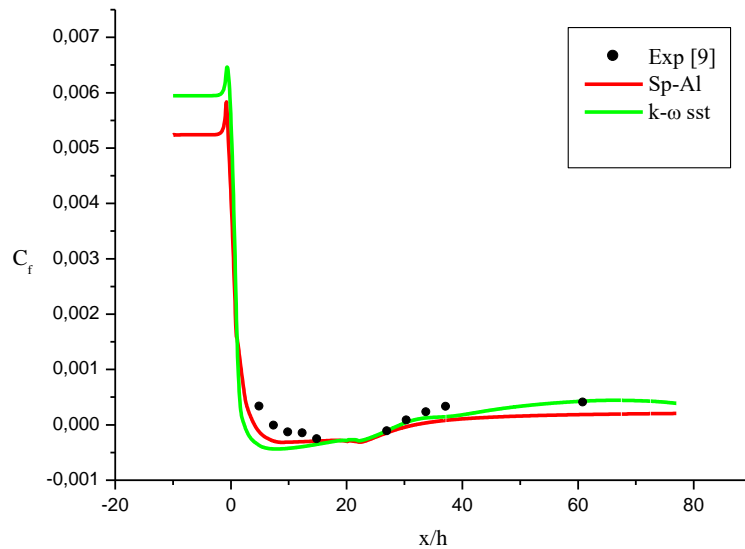


Fig. 5. Comparison of parietal friction coefficient  $C_f$  of the lower wall.

Figure 7 shows the comparison of the normalized axial velocity profiles by the velocity  $U_b$  taken for different positions  $x/h = -6, 3, 6, 14, 17, 20, 24$  and  $29$ . The experimentally predicted separation point is located at  $x/h$  equal to  $7.4$  while according to numerical calculations it is  $x/h$  equal to  $4.56$  for the best result obtained by the model Spalart-Allmaras.

The size of the bubble also grows much more slowly in the downward direction than the measured one. The measured re-attachment point is located at  $x / h$  equal to 29.2 while the calculated re-attachment point is at  $x / h$  equal to 31. In general, both models predict adequately the axial velocity in the majority of sections selected with the exception of  $x / h = 20$  where the difference between the numerical results and the experimental data is relatively large.

The size of the bubble also grows much more slowly in the downward direction than the measured one. The measured re-attachment point is located at  $x / h$  equal to 29.2 while the calculated re-attachment point is at  $x / h$  equal to 31. In general, both models predict adequately the axial velocity in the majority of sections selected with the exception of  $x / h = 20$  where the difference between the numerical results and the experimental data is relatively large.

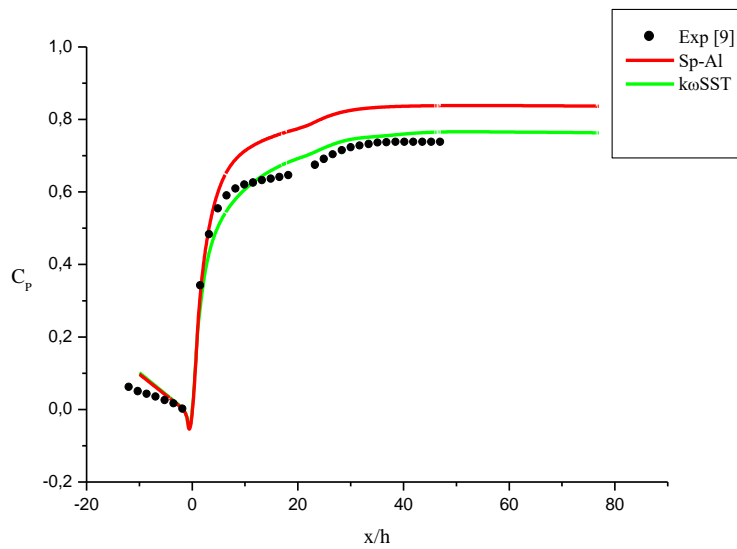
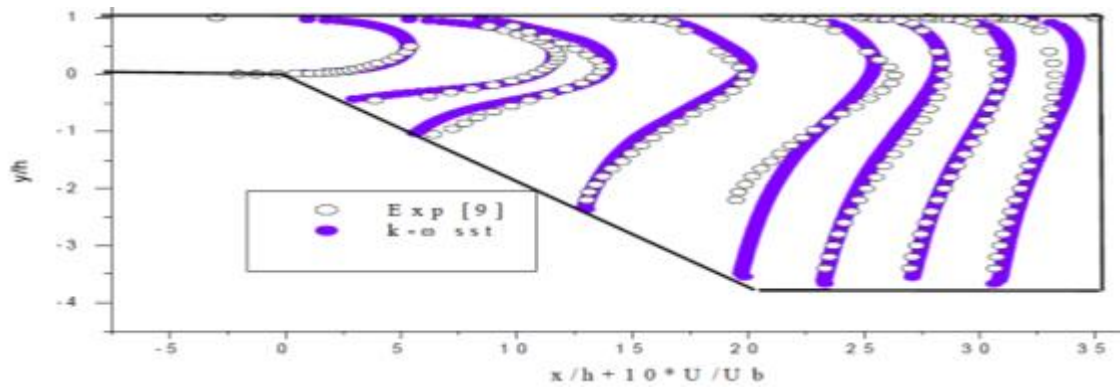


Fig. 6. Comparison of the pressure coefficient  $C_p$  on the lower wall.



a- Spalart-Allmaras Model

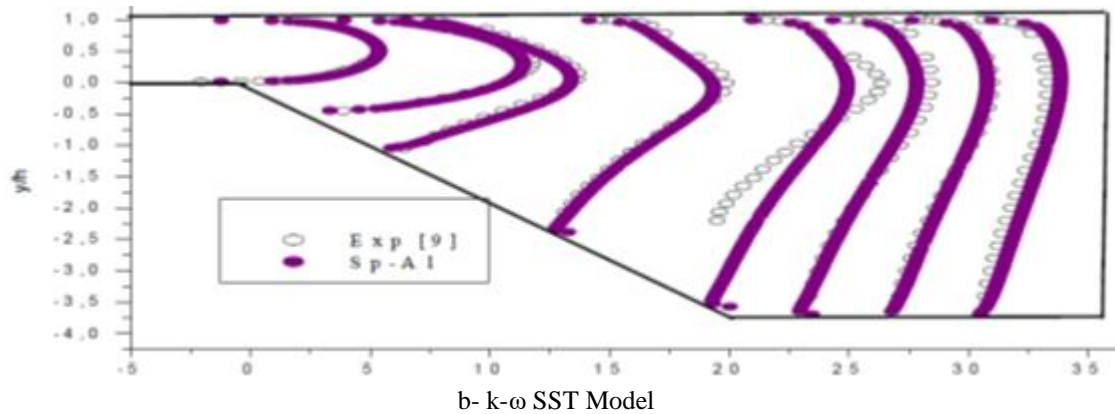


Fig. 7. Axial velocity distribution in the diffuser.

### Effect of the angle

The axial velocity contours are shown in figure 8, for a Reynolds number of 20,000 and different angles ranging from 6 ° to 16 °. It should be noted that blue areas represent axial velocities in the flow backflow region. The numerical results prove that the influence on the size of the separation bubble for turbulent flow is evident with the change of the angle of inclination. It is quite clear that the separation bubble size is proportional to the expansion angle. The separation zone tends to widen more and more for diffusers with a high expansion angle.

The distributions of the pressure coefficient along the direction of flow are shown in figure 9. The pressure coefficient is defined as:

$$C_p = \frac{C_{pw} - C_{pw(x/h=-1.7)}}{\frac{1}{2}\rho U_b^2} \quad (8)$$

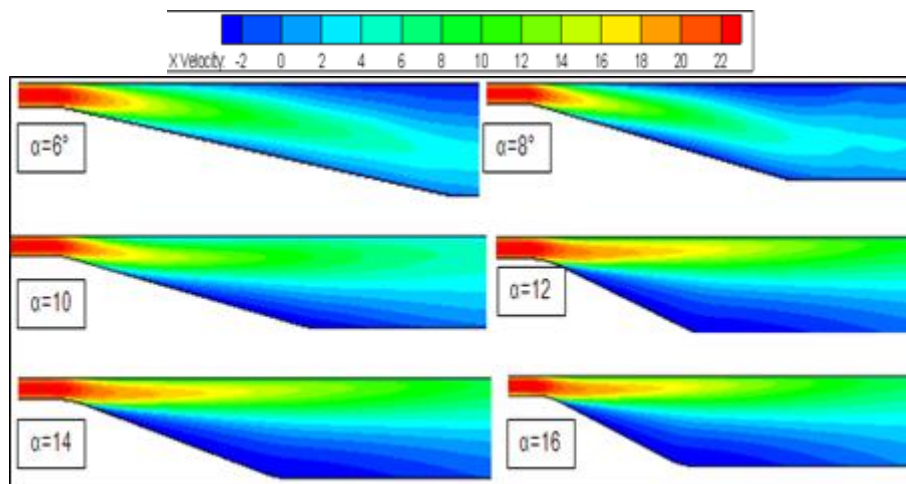


Fig. 8. Contour axial velocity for Re = 20000.

It is shown that the pressure coefficient increases in the diffuser and reaches its maximum value downstream of the diffuser at about  $x/h = 15$ . Here, the pressure coefficient is defined as the pressure recovery coefficient. It can be seen that it decreases with increasing diffuser angles for the Sp-A1 turbulence model. Increasing the diffuser angle to 16 degrees, the predictions for both turbulence models are quite smaller than that of the small angle diffuser.

It is suggested that separation does not occur until the divergence angle reaches 10 degrees. For diffuser angles of 14 and 16 degrees, the simulations proved that the separation caused a large pressure drop in the diffuser.

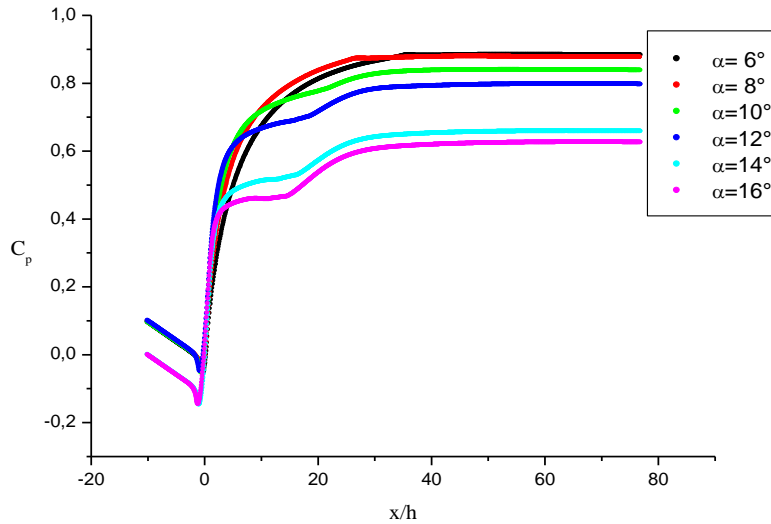


Fig .9. Effect of variation of tilt angle for Reynolds number 20000.

### Effect of Reynolds number

The systematic study of the influence of the Reynolds number on the flow structure for the diffuser angle of  $10^\circ$  shows the presence of the separation on the lower wall of the diffuser for Reynolds numbers 10000, 15000, 20000, 25000 and 30000 as shown in figure 10. The size of the recirculation zone is proportional to the variation of the Reynolds number, where we notice that the separation zone takes the narrowed form for Re equal to 10000. For Reynolds numbers from 15000 to 30000, an increase of the separation bubble is well noticed.

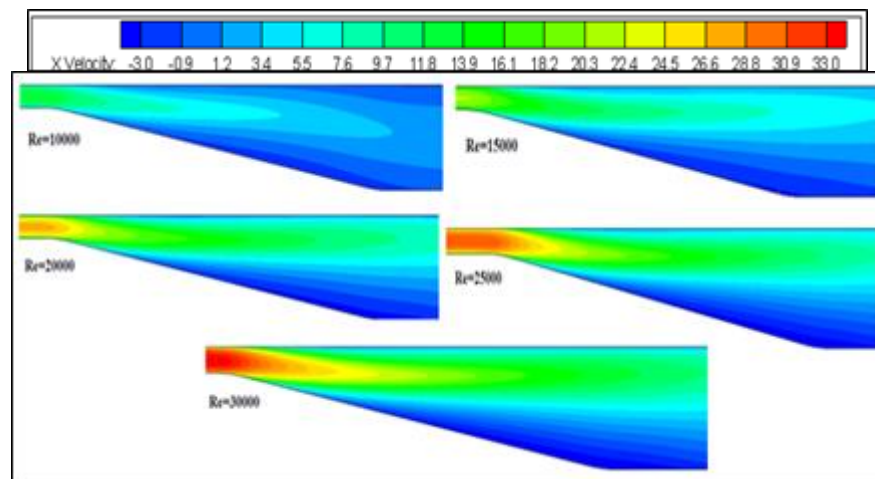


Fig. 10. Contour of the axial speed for the angle of 10.

Pressure coefficient distributions for Reynolds numbers from 10,000 to 30,000 for the Sp-AI model are shown in figure 11. It is found that the pressure coefficient increases when the Reynolds number increases for the angle of  $10^\circ$ . For the Reynolds number ranging from 10,000 to 25,000, the differences in pressure coefficient distribution are not so obvious. A

more detailed analysis shows that the increase in the Reynolds number can affect the performance of the diffuser at Re equal to 30,000, where a noticeable rise in the pressure coefficient is noted.

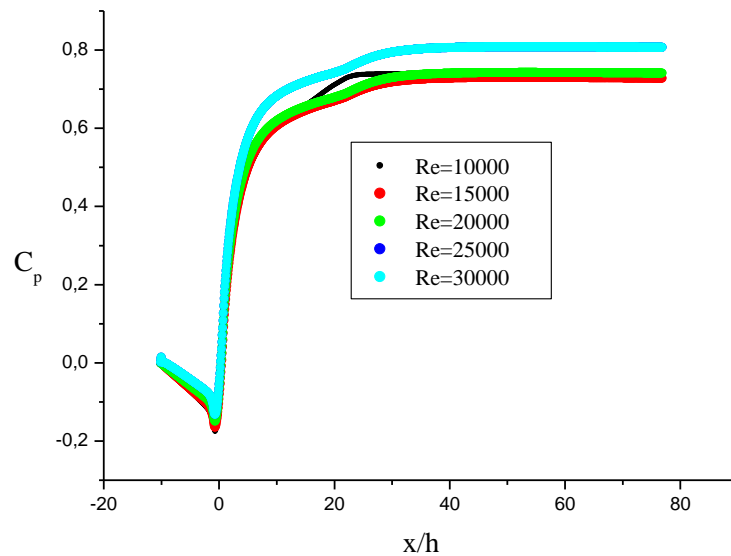


Fig.11 Effect of variation of Reynolds number at 10 ° angle.

## CONCLUSION

The present study is a numerical contribution to the study of turbulent flow separation in an asymmetric subsonic plane diffuser. The intended goal is to identify the best turbulence model capable of predicting separation and re-attachment as accurately as possible compared to experimental data from (Buice, 1997). Numerical simulations were carried out in 2D through the resolution of the differential equations using the ANSYS Fluent commercial code. The flow considered is fully developed at the entrance with a Reynolds number of the order of 20000.

For the closure of the system of equations, three models were used: the one-equation model Spalart-Allmaras, the model  $k-\omega$  SST, and the model with five equations RSM. In addition to testing the turbulence models, the effects of grid resolution were also examined by varying the number of points in the vertical direction and also the thickness of the first cell at the wall to control the  $y^+$  between 5 and 30.

It turned out that the results of the Spalart-Allmaras and  $k-\omega$  SST models are in good agreement with the literature.

Parametric studies were conducted to demonstrate the influence of the diffuser angle and Reynolds number on the separation of the flow in the diffuser. Several tests have been done to answer this question. The simulations were performed for angles of divergence ranging from 6 to 16 with a step of 2 °. For each divergence angle, the Reynolds number at the diffuser input was set at 20,000. It was found that the influence of the inclination on the size of the recirculation region is directly proportional to the angle of inclination, so we can note the abstention of this phenomenon for angles below 8°. It is suggested that separation does not occur until the angle of divergence reaches 10°.

It has also been found that the influence of inclination on the size of the recycle region for turbulent flow is evident with the change of diverging angles.

The effect of Reynolds number on boundary layer separation at an expansion angle of 10 ° was also performed. The simulations showed that the separation occurred for all the Reynolds numbers experienced only it remained practically unchangeable in terms of size.

## 12 REFERENCES

- Buice, C. U., Experimental Investigation of flow through an asymmetric plane diffuser , Ph.D. thesis, Stanford University, Stanford, CA, Aug. 1997.
- DalBello T., Dippold V., Georgiadis N. J., 2005. Technical Report. WBS 22-781-30-70. NASA Glenn Research Center; Cleveland, OH, United States. Unclassified; Publicly available; Unlimited.
- Davidson L., 2005. MTF071 Lecture notes. Charlmers University of Technology, Goteborg, Sweden.
- Iaccarino, G. (2001). Predictions of a turbulent separated flow using commercial CFD codes. *Journal of Fluids Engineering, Transactions of the ASME*, 123(4). <https://doi.org/10.1115/1.1400749>
- Kaltenbach, H. J., Fatica, M., Mittal, R., Lund, T. S., & Moin, P. (1999). Study of flow in a planar asymmetric diffuser using large-eddy simulation. *Journal of Fluid Mechanics*, 390. <https://doi.org/10.1017/S0022112099005054>
- Obi, S., Aoki, K., & Masuda, S. (1993). Experimental and computational study of turbulent separating flow in an asymmetric plane diffuser. *Proc. 9th Symposium on Turbulent Shear Flows*.
- Obi, S., Ohizumi, H., Aoki, K., & Masuda, S. (1993). Turbulent separation control in a plane asymmetric diffuser by periodic perturbation. In *Engineering Turbulence Modelling and Experiments*. <https://doi.org/10.1016/b978-0-444-89802-9.50064-2>
- Tornblom O., 2003. Technical Reports from Royal Institute of Technology Department of Mechanics SE-100 44 Stockholm, Sweden.